Available online at www.sciencedirect.com

SciVerse ScienceDirect

Ceramics International 39 (2013) 745–752

CERAMICS INTERNATIONAL

www.elsevier.com/locate/ceramint

The effect of antimony trioxide on poly (vinyl alcohol)-lithium perchlorate based polymer electrolytes

Chin-Shen Lim, S. Ramesh*, S.R. Majid

Centre for Ionics University of Malaya, Department of Physics, Faculty of Science, University of Malaya, Lembah Pantai, 50603 Kuala Lumpur, Malaysia

Received 24 May 2012; received in revised form 27 June 2012; accepted 27 June 2012
Available online 27 July 2012

Abstract

A new type of inorganic filler antimony trioxide (Sb_2O_3) is used to prepare composite polymer electrolytes based on poly (vinyl alcohol) (PVA) and lithium perchlorate ($LiClO_4$) by solution casting technique. The incorporation of Sb_2O_3 enhances the ionic conductivity at ambient temperature and exhibits the highest ionic conductivity value of 9.51×10^{-5} S cm^{-1} upon the addition of 6 wt% Sb_2O_3. Thermogravimetric analyses (TGA) reveal that the second weight loss is reduced. This shows the improvement in thermal stability of electrolyte film upon addition of Sb_2O_3. Differential scanning calorimetry (DSC) analyses show that the glass transition temperature (T_g) value decreases with incorporation of Sb_2O_3. X-ray diffraction (XRD) studies show that the addition of Sb_2O_3 decreases the degree of crystallinity whereas scanning electron microscope (SEM) studies reveal the surface morphology of the prepared composite polymer electrolytes.

Keywords: C. Ionic conductivity; Antimony trioxide; Poly (vinyl alcohol)

1. Introduction

Since the last two decades, solid polymer electrolytes have emerged as a potential material for application in electrochemical devices due to special properties such as good electrode–electrolyte contact, ease of preparation in different forms as well as good mechanical and adhesive properties. Polymer complexes with inorganic salts have widely developed because of their application in the development of batteries, electrochromic devices and electrochemical sensors [1,2]. Solid polymer electrolytes are preferred compared to gel polymer electrolytes and liquid polymer electrolytes as solid polymer electrolytes have high energy density, are leak proof, solvent-free, have wide electrochemical stability windows, simplified processability and light weight compared to gel polymer electrolytes.

Several studies have reported poly (ethylene oxide) PEO as having ionic conduction characteristics [3,4]. However, in the study of PEO–LiX ($X = ClO_4^-$, $CF_3SO_3^-$, BF_4^-, PF_6^- etc.), the polymer electrolyte does not attain high lithium ionic conductivity at ambient temperature. In addition, PEO exhibits poor mechanical properties that reduces the ease of fabrication. One way to enhance the ionic conductivity and mechanical properties is to incorporate inorganic filler. Incorporation of inorganic fillers like Al_2O_3, TiO_2, $BaTiO_3$ and SiO_2 into PEO based polymeric complexes has shown enhancement in ionic conductivity [5–8]. The addition of inorganic fillers to the polymer–lithium salt systems generally improves the transport properties, resistance to crystallization, and stability of the electrode–electrolyte interface. Thus, the addition of inorganic fillers to polymer matrix is to promote more free ions and to increase the amorphous nature of the complexes which will lead to a higher ionic conductivity value. Basically, the enhancement of ionic conductivity of polymer electrolytes through addition of inert filler can be explained in terms of disruption of crystallization in the polymer matrix [9,10]. Apart from that, plasticized polymer electrolytes show poor mechanical properties and higher reactivity towards lithium anode. This explains why many researchers have tried to retain the mechanical properties and thermal

*Corresponding author. Tel: +60 3 79674146.
E-mail address: rameshtsubra@gmail.com (S. Ramesh).

0272-8842/$ - see front matter © 2012 Elsevier Ltd and Techna Group S.r.l. All rights reserved.
http://dx.doi.org/10.1016/j.ceramint.2012.06.087

stability of polymer electrolytes through the introduction of inert filler [11–13]. The addition of filler shifts the degradation temperature to a higher temperature meaning that the polymer electrolyte is more heat resistant. This indicates the improvement in thermal stability of the electrolytes [14,15].

In this study, a new type of inorganic filler, Sb_2O_3, has been incorporated into the polymer–salt system. Sb_2O_3 is an amphoteric oxide where the molecules are able to react as an acid as well as a base. In addition, Sb_2O_3 has the ability to increase the ionic conductivity of polymer electrolytes. The purpose of this work is to study the effect of Sb_2O_3 on the PVA–$LiClO_4$ system. Characterization was carried out by impedance spectroscopy, thermogravimetry (TGA), differential scanning calorimetric (DSC), X-Ray diffraction (XRD) and scanning electron microscope (SEM) to study the effect of Sb_2O_3 on polymer electrolytes.

2. Experimental

PVA (Aldrich, 99% hydrolyzed), $LiClO_4$ (Merck) and Sb_2O_3 (Aldrich, < 250 nm particle size) were used as received without further treatment or purification. For this study, thin films consisting of PVA, $LiClO_4$ and Sb_2O_3 were prepared by solution casting technique with distilled water as solvent. The PVA and $LiClO_4$ were mixed and stirred at 85 °C for 1 h until a homogenous solution is obtained before adding Sb_2O_3. The mixture was stirred for several hours to allow the Sb_2O_3 to disperse well in the solution. The solution was then cast in a petri dish and allowed to evaporate slowly in the oven at 70 °C. This procedure yields mechanically stable and free-standing films. Designations of polymer electrolytes with the various percentage of Sb_2O_3 added are presented in Table 1. The thickness of the films was measured by means of a micrometer screw gage. The films were sandwiched between two stainless-steel blocking electrodes. The ionic conductivity of the samples was measured by using HIOKI 3532-50 LCR Hi-tester with the AC frequency in the range from 50 Hz to 5 MHz and from room temperature to 80 °C. DSC analysis was carried out using TA instrument Q200. Nitrogen purge gas was used with 50.0 ml min^{-1} flow rate. Sample with approximately 5 mg was sealed in a 40 μl aluminum crucible. Before analysis, the samples were equilibrated at 105 °C for 5 min to remove any traces of water. The samples were then cooled rapidly to −50 °C and then reheated to 180 °C at 30 °C min^{-1}. TGA analysis was carried out using TA instrument Q500 with the heating rate of 10 °C/min between 30 °C and 400 °C in nitrogen gas atmosphere. XRD analysis was carried out to investigate the crystalline nature of the polymer electrolytes. The XRD patterns were recorded on a Siemens D 5000 diffractometer with Cu-Kα radiation ($\lambda = 1.54060$ Å), over the range of $2\theta = 5$–80° at ambient temperature. The crystallite size of Sb_2O_3 has been calculated from the Scherrer equation [16]:

$$L = \frac{0.9\lambda}{\beta \cos\theta}$$

where λ is the wavelength of the impinging X-ray beam, β is the full width at half maximum intensity of the XRD peak and θ is the glancing angle. Morphology of composite polymer electrolyte was recorded by means of Leica's SEM instrument model S440 and examined at 10 kV at room temperature.

Table 1
Designation and composition of composite polymer electrolytes.

Designation	Composition (PVA:$LiClO_4$:Sb_2O_3)
PLS-0	60:40:0
PLS-2	58.8:39.2:2
PLS-4	57.6:38.4:4
PLS-6	56.4:37.6:6
PLS-8	55.2:36.8:8
PLS-10	54:36:10

3. Results and discussion

3.1. Room temperature ionic conductivity studies

Ionic conductivity of solid polymer electrolytes was calculated from the impedance plot using the following equation:

$$\sigma = \frac{L}{R_b A}$$

where L, A and R_b, are the thickness, area and bulk resistance of the solid polymer electrolytes, respectively. Fig. 1 depicts the typical impedance plot of PLS-6 at room temperature. The semicircle fitting was achieved to obtain the R_b value. As shown in Fig. 1, R_b is determined from interception of the semicircle and the spike at x-axis.

The relationship between Sb_2O_3 content and the ionic conductivity of the polymer electrolytes is shown in Fig. 2. The ionic conductivity of an electrolyte depends on the number of charge carriers and their mobility in the electrolyte is often defined as follows:

$$\sigma = \sum n_i z_i \mu_i$$

where n_i, z_i and μ_i represent the number of charge carriers, the ionic charge and the ionic mobility respectively. Fig. 2 shows that the ionic conductivity of the polymer electrolyte increases gradually as the weight percentage of Sb_2O_3 is increased up to 6 wt%. This is due to the increase in the number of charge carriers, n_i with the addition of Sb_2O_3 and it can be concluded that the filler aids to dissociate the lithium salt more easily. Mobility of Li^+ is enhanced by reduction of the tendency of Li^+ coordinate with the oxygen atom in PVA.

Sb_2O_3 also has the ability to penetrate into the polymer matrix and promotes an interaction between Sb_2O_3, $LiClO_4$, and PVA chains. Consequently, the cohesive force between the polymer chains is reduced which provides a

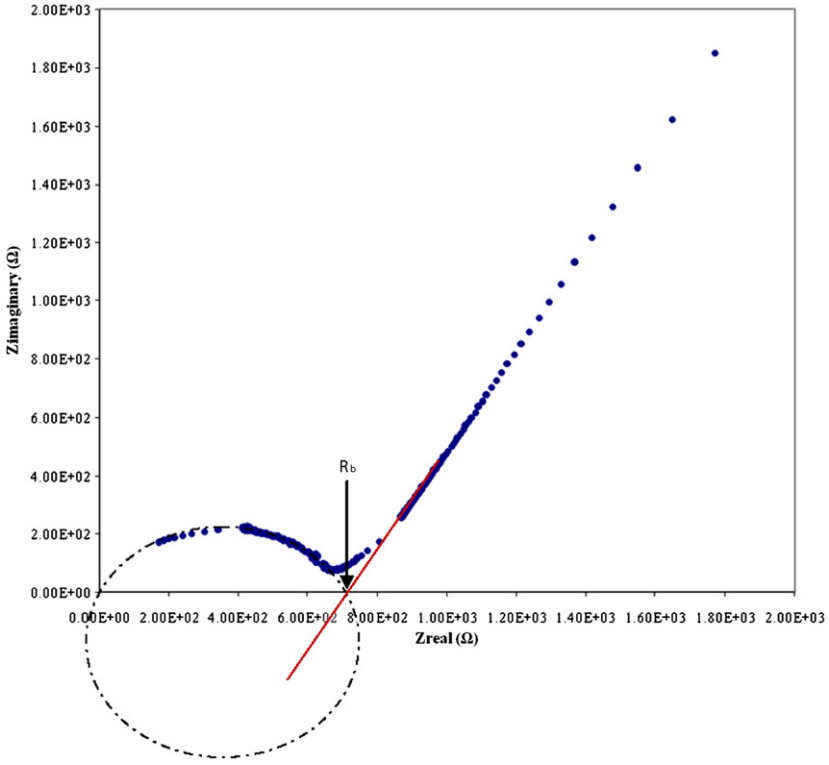

Fig. 1. Impedance spectrum for PLS-0 at room temperature.

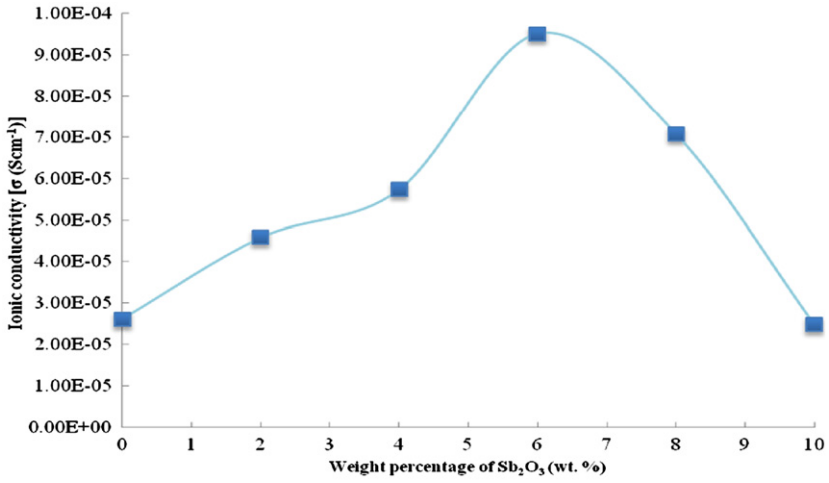

Fig. 2. The variation of ionic conductivity values as a function of Sb_2O_3 concentration.

more flexible chain segmental motion [17]. Moreover, the active sites on the Sb_2O_3 surface aid in lowering the ionic coupling and dissociate the $LiClO_4$ aggregate into free charge carriers [18]. In addition, Lewis acid–base type oxygen and OH surface groups on the antimony grains interact with the charge carriers (cation and anion). This provides cross-linking centers for PVA segment and anions. This modifies the network structure, leading to lowering of PVA reorganizing tendency and promoting cation-conducting pathways along the filler surface within the network. The creation of Lewis acid–base centers with ionic species results in the ease of dissociation of lithium salt. This will increase the number of charge carriers as well as ionic conductivity [19,20]. The disperse fillers which may act as 'solid plasticizers' are capable of enhancing the composite polymer electrolyte's transport properties without affecting its mechanical and interfacial stability.

PLS-6 exhibits the highest ionic conductivity value of 9.51×10^{-5} S cm^{-1} at ambient temperature. However, as the weight percentage of nanosized Sb_2O_3 increased up to 8 wt%, the ionic conductivity of the polymer electrolytes starts to drop. This can be attributed to the aggregation of Sb_2O_3 nanoparticles leading to blocking effect on conducting pathway, hence immobilizing the polymer chain [21].

3.2. Temperature dependence ionic conductivity studies

The temperature dependence of the ionic conductivity measurement was carried out to study the mechanism of ionic conduction for PVA:$LiClO_4$:Sb_2O_3 samples. Fig. 3 indicates the Arrhenius plot for various compositions of polymer electrolytes at different temperatures. The linear relationship between log ionic conductivity and reciprocal temperature suggests that all the samples obeyed the Arrhenius rule, as their regression value is approximately unity. Hence, the temperature dependent conductivity can be expressed by the Arrhenius equation:

$$\sigma = A \exp\left(-\frac{E_a}{kT}\right)$$

where A is a constant which is proportional to the amount of charge carriers, E_a is the activation energy, k is the Boltzmann constant and T represents the absolute temperature in K. Fig. 3 shows that the ionic conductivity of samples increased with increase in temperature. As temperature increases, polymer chain acquires faster internal modes in which hopping mechanism is favored. The rise of temperature increases the rate of hopping mechanism, which in turn enhances the mobility of ions. The coordination site of PVA for Li^+ is oxygen atom; the interactions between these two atoms had been weakened by the increase in temperature that causes the Li^+ to be loosely bound to the oxygen atom. At higher temperature, the backbone of the polymer has a higher tendency to create vacant sites where the adjacent site of ions will then occupy [22].

The activation energy, E_a, value for PLS-0, PLS-2, PLS-6 and PLS-8 is 20.6 kJ mol^{-1}, 19.6 kJ mol^{-1}, 16.8 kJ mol^{-1} and 19.4 kJ mol^{-1} respectively, which is highly dependent on the content of Sb_2O_3. The E_a value for PVA–$LiClO_4$–Sb_2O_3 composite polymer electrolyte is of the order of $16.8-20.6$ kJ mol^{-1}. Yang [23] reported that the E_a value for polymer electrolyte without inorganic filler is 20 kJ mol^{-1}. After incorporation of inorganic filler into polymer matrix, E_a value slightly decreases which may be due to lesser energy to weaken the dipole–dipole interaction. The E_a value decreases with increase in the content of Sb_2O_3. The PLS-6 has lower E_a value compared to PLS-0 and PLS-2; this infers that PLS-6 requires lesser energy to break the physical and chemicals bonds and, therefore ionic conduction is more favorable on PLS-6 sample. On the other hand, E_a value for PLS-8 is found to increase. This can be attributed to the formation of aggregates and ion pairs which require higher energy to weaken the coordinative bonds in the polymer matrix.

3.3. DSC studies

In this study, DSC was used to determine the glass transition temperature (T_g). In general, a low glass transition temperature enhances the amorphous nature of the polymer as well as the flexibility. The flexibility of the polymeric chain is directly related to the glass transition temperature (T_g). The lower the value of T_g, the higher the flexibility of the polymeric chains or segments. Fig. 4 depicts the plot of DSC curves for pure PVA, PLS-0, PLS-2, PLS-6 and PLS-8 in the temperature range of 30–180 °C. The endothermic reaction of T_g can be observed in Fig. 4. No melting temperature (T_m) exists in the DSC plot, which means that the polymer electrolyte shows amorphous structure in the temperature range of 30–180 °C as lithium ionic transport takes place in the amorphous phase. Table 2 shows the glass transition temperature of PVA, PLS-0, PLS-2, PLS-6 and PLS-8. The glass transition of PVA obtained from DSC analysis is 80.2 °C. The transition temperature shifts from 80.2 °C to 84.2 °C upon the addition of $LiClO_4$. This phenomenon indicates that the solvation of the lithium cation with the oxygen atom of the PVA is partially interrupted with the local motion of the polymer segment through the formation of transient crosslink of rotation. This causes an increase in T_g value [24]. Hence, it can be said that the solvation of Li^+ reduces the flexibility of the polymer chain.

Incorporation of 2 wt% of Sb_2O_3 into the polymer system indicates no appreciable change in the T_g as shown

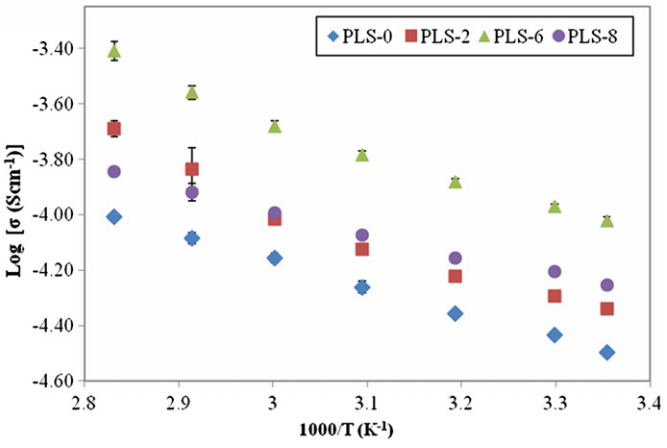

Fig. 3. Arrhenius plots of ionic conductivity of PLS-0, PLS-2, PLS-6 and PLS-8.

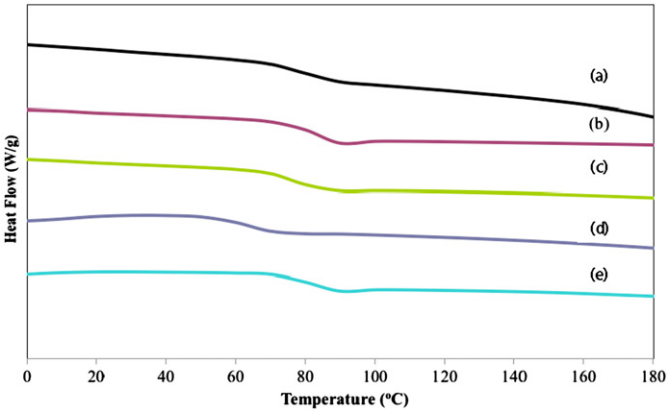

Fig. 4. DSC thermograms of (a) pure PVA, (b) PLS-0, (c) PLS-2, (d) PLS-6 and (e) PLS-8.

Table 2
Glass transition temperature (T_g) in DSC analyses and Total weight loss (%) in TGA analyses for composite polymer electrolytes.

Sample	T_g (°C)	Total weight loss (%) at temperature range of 210–280 °C
PLS-0	84.2	29.07
PLS-2	79.6	23.11
PLS-6	72.1	26.73
PLS-8	82.9	25.33

in Table 2. It can be concluded that T_g is not influenced by the low content of Sb_2O_3. When the weight percentage of Sb_2O_3 is increased to 6 wt%, the glass transition of the polymer shifts to a lower temperature value of 72.1 °C. The shifting of T_g suggests that there is an interaction between Sb_2O_3 and polymer backbone. PLS-6 obtains the lowest glass transition temperature compared to other samples. This is due to addition of Sb_2O_3 that weakens the dipole–dipole interactions, which enable the easy flow of ions through polymer chains network when there is an applied electric field compared to other samples [25]. As T_g lowers, the amorphous phase becomes more flexible and provides fast ion conduction, hence increasing the ionic conductivity of polymer electrolyte. This implies that the addition of Sb_2O_3 has enhanced the ionic conductivity of the polymer electrolytes.

As the weight percentage of Sb_2O_3 is increased to 8 wt%, T_g shifts to a slightly higher temperature of 82.9 °C. The increase in T_g with the addition of Sb_2O_3 is due to the stiffening of the polymeric segments, thereby suppressing the polymeric chain motion. Hence ionic conductivity of polymer electrolyte decreases.

3.4. TGA studies

In this study, TGA was employed to study the thermal stability of the polymer electrolytes. Fig. 5 illustrates the TGA thermograph of PVA, PLS-0, PLS-2, PLS-6 and PLS-8. The PVA film shows two major weight loss regions. There is a weight loss of 7% from 70 °C to 100 °C for the pure PVA. This is due to the evaporation of the weakly physical yet strongly chemical bound H_2O or elimination of impurities [26]. The second weight loss occurring at around 218 °C is due to the decomposition of PVA film with the weight loss of 37.36%. In addition, the weight loss of PVA also increases as the temperature increases from 250 °C to 300 °C. This might be attributed to the carbonation [27].

PLS-0, PLS-2, PLS-6 and PLS-8 also show two stages of weight loss. First stage of the weight loss is attributed to the evaporation of free and bound water. The weight loss of polymer electrolytes for the first stage had increased upon the addition of $LiClO_4$. $LiClO_4$ is a hygroscopic substance and has the ability to absorb water from its surroundings, increasing the weight loss for PLS-0, PLS-2, PLS-6 and PLS-8 as shown in Fig. 5.

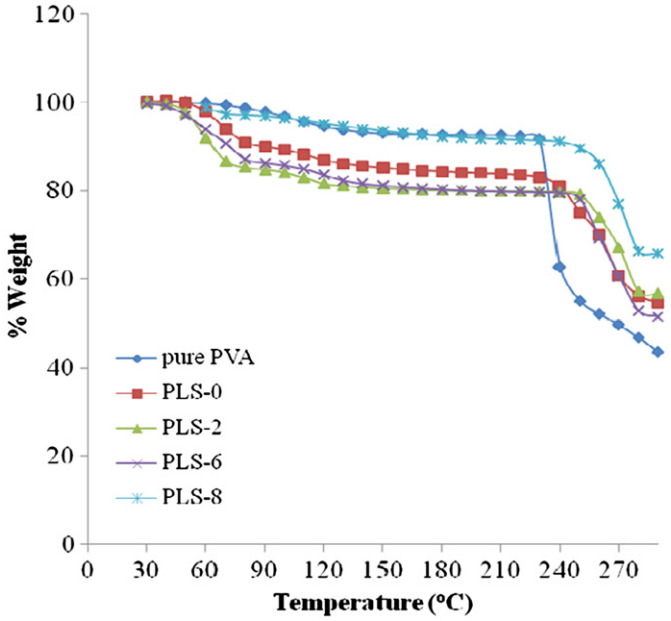

Fig. 5. Thermogravimetric curves of PLS-0, PLS-2, PLS-6 and PLS-8.

Fig. 5 also shows that there is a second weight loss for PLS-0, PLS-2, PLS-6 and PLS-8 at the temperature range of 210–280 °C. The onset decomposition temperature has shifted towards higher temperature upon the addition of $LiClO_4$ and Sb_2O_3. The onset decomposition temperature of PLS-0 is found to be approximately 240 °C whereas onset decomposition temperature of PLS-2, PLS-6 and PLS-8 is approximately 250 °C. The addition of Sb_2O_3 has enhanced the thermal stability of the polymer membrane where PLS-2, PLS-6 and PLS-8 undergo decomposition at higher temperature.

The total percentage of weight loss at 210–280 °C for PLS-0, PLS-2, PLS-6 and PLS-8 is tabulated in Table 2. Results show that the addition of Sb_2O_3 to the system had reduced the percentage of weight loss. This infers that the thermal stability of polymer electrolytes increased upon the incorporation of Sb_2O_3. These composite polymer electrolytes have become more thermally stable and more resistant to heat as compared to polymer electrolytes without filler.

3.5. XRD studies

X-ray diffraction measurements were performed to investigate the structural properties of the PVA based complexed polymer electrolytes. Fig. 6 shows the XRD diffractogram of PVA, Sb_2O_3 and $LiClO_4$. From Fig. 6(a), the crystalline peak of PVA is obtained at glancing angles of $2\theta = 19.8°$ which reveals the semi-crystalline nature of PVA. The crystalline peaks for Sb_2O_3 at angles of $2\theta = 25.3°$, 28.4°, 44.2°, 50.3° and 54.4° are shown in Fig. 6(b). The crystalline peaks for $LiClO_4$ was obtained

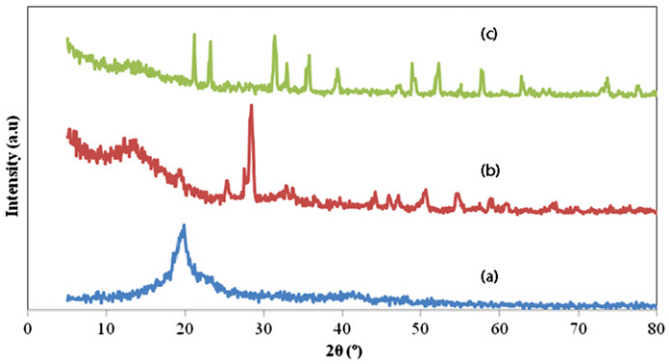

Fig. 6. XRD patterns of (a) PVA, (b) Sb_2O_3 and (c) $LiClO_4$.

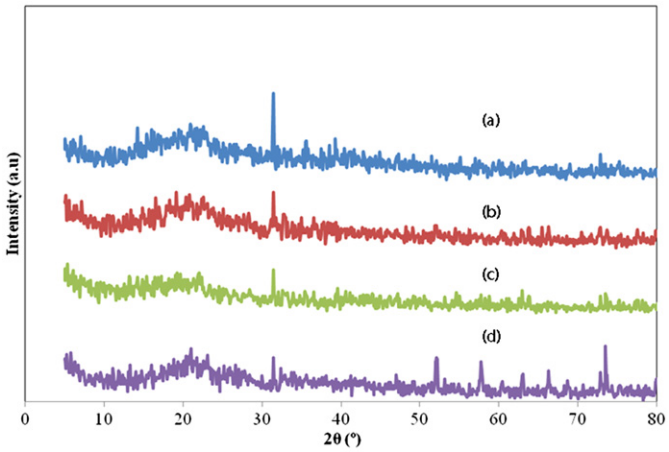

Fig. 7. XRD patterns of (a) PLS-0, (b) PLS-2, (c) PLS-6 and (d) PLS-8.

at angles of $2\theta = 21.1°$, 23.2°, 31.3°, 31.4°, 35.7° and 39.3° as depicted in Fig. 6(c).

Fig. 7 reveals the XRD pattern of PLS-0, PLS-2, PLS-6 and PLS-8. Results show that the relative peak at $2\theta = 19.8°$ for pure PVA had shifted to $2\theta = 19.5$, 19.4, 19.0 and 19.3 in PLS-0, PLS-2, PLS-6 and PLS-8, respectively. The shifting of peaks is attributed to the incorporation of $LiClO_4$ and Sb_2O_3. This phenomenon shows that complexation has occurred between PVA, $LiClO_4$ and Sb_2O_3. The peak intensity of relative diffraction peak is an indicator to study the structural characteristic of polymer electrolytes. As the peak intensity of relative diffraction peak becomes lower and broader, the polymer electrolytes have more amorphous characteristic, hence enhancing the ionic conductivity [28,29].

PLS-0 indicates decrease in intensity of the crystalline peak of PVA at $2\theta = 19.8°$ upon the addition of $LiClO_4$. This implies that the addition of $LiClO_4$ disrupted the arrangement in the polymer backbone of PVA. There is an intense peak present for PLS-0 sample at $2\theta = 30.3°$ that corresponds to the crystalline peak of $LiClO_4$. This is because $LiClO_4$ does not undergo complete dissolution in the polymer matrix. Addition of 2 wt% Sb_2O_3 does not show any significant changes in relative peak intensity. This implies that small amount of filler does not enhance the degree of amorphousness of the sample. The relative peak intensity of PVA had become slightly less intense with further addition of 6 wt% and 8 wt% of Sb_2O_3 which implies that the amorphous nature of the polymer electrolyte is enhanced. This, in turn enhances the polymer chain flexibility as well as the ionic conduction. Fig. 7 indicates that PLS-6 has more amorphous character compared to other samples. By comparing to Fig. 7(c) and (d), the relative peak intensity for PLS-6 is observed to be less intense than PLS-8. Few crystalline peaks were present from the XRD diffractogram with further addition of Sb_2O_3 up to 8 wt%. This is attributed to excessive amount of Sb_2O_3 that does not undergo complexation with the PVA–$LiClO_4$ matrix.

Results also shows that Sb_2O_3 decreases the intensity of crystalline peak at $2\theta = 30.3°$ which corresponds to $LiClO_4$. This behavior shows that lithium salt dissociates into free charge carrier upon the addition of Sb_2O_3, which is in good agreement with ionic conductivity studies.

The calculated crystallite size for PLS-0, PLS-2, PLS-6 and PLS-8 is 46.9 Å, 28.1 Å, 2.1 Å and 23.4 Å respectively. Based on Scherrer equation, the higher the value of FWHM, the smaller the crystallite sizes. Addition of Sb_2O_3 had reduced the crystallite size as well as the crystallinity of the polymer electrolytes. PLS-6 which gives the highest ionic conductivity has the smallest crystallite size. The crystallite size was increased with the incorporation of 8 wt% Sb_2O_3 due to excessive amount of filler content. This is attributed to the formation of aggregates. This is proven by the existence of the crystalline for PLS-8 as shown in Fig. 7(d).

3.6. SEM studies

The crystallite size of polymer electrolytes can be further validated by referring to SEM micrographs. The surface morphology of PLS-0, PLS-2, PLS-6 and PLS-8 is shown in Fig. 8. Fig. 8(a) shows the SEM image of PVA–$LiClO_4$ without Sb_2O_3. The surface morphology is uniform and no phase separation is seen. This infers an excellent distribution of lithium salt in the polymer matrix. Thus complexation between PVA and $LiClO_4$ is confirmed. Upon the addition of Sb_2O_3, the particles of Sb_2O_3 are well dispersed on polymer matrix and uniform throughout the surface of polymer matrix. This complexation between filler and polymer host is revealed in SEM micrographs, where the shape of particle or surface morphology is altered compared to polymer electrolyte without filler as shown in Fig. 8(a).

The dispersed Sb_2O_3 particles play an active role in the growth of microstructures resulting in different morphology. PLS-2 and PLS-8 have larger crystallite size compared to PLS-6 as shown in Fig. 8. Coagulation that happen in PLS-2 is attributed to the small amount of filler that does not disperse separately whereas formation of aggregates in PLS-8 is due to excessive amount of Sb_2O_3 that has been added. The ionic conductivity of PLS-2 and PLS-8 is not affected by coagulation and aggregates as the formation of

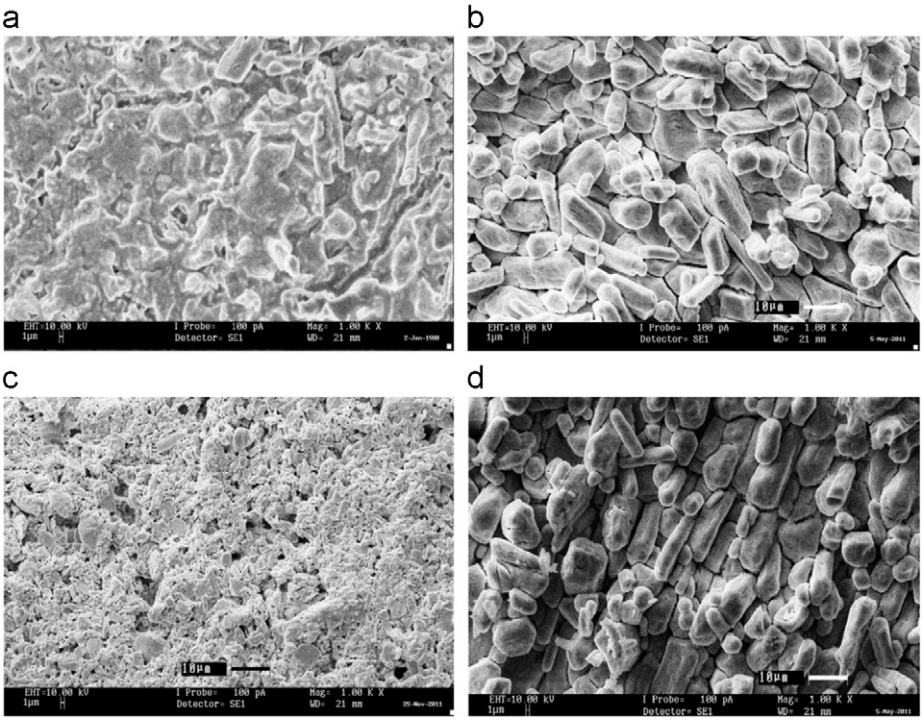

Fig. 8. SEM images of (a) PLS-0, (b) PLS-2, (c) PLS-6, and (d) PLS-8.

voids can be seen in the SEM images. Formation of voids creates conducting pathway in the polymer matrix and enhances the mobility of ions. Eventually, it increases the ionic conductivity. PLS-6 exhibits the highest ionic conductivity; this is ascribed to small crystallite size that results in higher surface area. Small crystallites tend to create high void surface area compared to bulk crystallites. This will ease the Li^+ ion to conduct in the polymer matrix. In terms of the number of voids, the higher the number of void, the more the conducting pathways created. Therefore, the ionic conductivity for PLS-6 increases. These results were in agreement with the ionic conductivity studies where PLS-6 exhibits the highest ionic conductivity.

4. Conclusion

The polymer electrolyte containing 6 wt% of Sb_2O_3 produces a free-standing film and exhibits the highest ionic conductivity of 9.51×10^{-5} S cm^{-1}. In addition, the polymer system obeys the Arrhenius relationship, as the regression value is approximately unity thus hopping mechanism is favored when temperature increased. PLS-6 shows the lowest T_g value based on DSC analysis. The flexibility of polymer electrolyte is enhanced and fast ion conduction is favored, thus the ionic conductivity increases. TGA analyses also inferred that the addition of Sb_2O_3 improves the thermal stability of the polymer complexes. XRD analyses have proven that the addition of Sb_2O_3 enhances the amorphous characteristic of polymer electrolyte as well as the ionic conductivity. The morphological studies showing the complexation between Sb_2O_3 and polymer electrolyte was revealed by SEM images.

Acknowledgment

This work was supported by the Exploratory Research Grant Scheme (ERGS: ER017-2011A) from Ministry of Higher Education, Malaysia and Universiti Malaya Research Grant (UMRG: RG140-11AFR).

References

[1] C.A. Vincent, Polymer electrolytes, Progress in Solid State Chemistry 17 (1987) 145.
[2] H.J. Walls, J. Zhou, J.A. Yerian, P.S. Fedkiw, S.A. Khan, M.K. Stowe, G.L. Baker, Fumed silica-based composite polymer electrolytes: synthesis, rheology and electrochemistry, Journal of Power Sources 89 (2000) 156.
[3] R. Frech, W.W. Huang, Polymer conformation and ionic association in complexes of lithium, sodium and potassium triflate with poly (ethylene oxide) oligomers, Solid State Ionics 72 (1994) 103–107.
[4] Y. Tominaga, H. Ohno, Lithium ion conduction in linear- and network-type polymers of PEO/sulfonamide salt hybrid, Electrochimica Acta 45 (2000) 3081–3086.
[5] F.M. Gray, in: Solid State Electrolytes, VCH Publisher, New York, 1991.
[6] W. Wiezoreck, J.R. Stevens, Z. Florjanczyk, Composite polyether based solid elecrolytes. The Lewis acid–base approach, Solid State Ionics 85 (1996) 67–72.
[7] S. Ramesh, Soon-Chien Lu, Effect of nanosized silica in poly(methyl methacrylate)-lithium bis(trifluoromethanesulfonyl)imide based polymer electrolytes, Journal of Power Sources 185 (2008) 1439–1443.
[8] M.A.K.L. Dissanayake, L.R.A.K. Bamdara, L.H. Karaluyadda, P.A.R.D. Jayathilaka, R.S.P. Bokalawala, Thermal and electrical properties of solid polymer electrolyte PEO_9 $Mg(ClO_4)_2$ incorporating nano-porous Al_2O_3 filler, Solid State Ionics 177 (2006) 343–346.

[9] S.H. Chung, Y. Wang, L. Persi, F. Croce, S.G. Greenbaum, B. Scrosati, E. Plichta, Enhancement of ion transport in polymer electrolytes by addition of nanoscale inorganic oxides, Journal of Power Sources 97–98 (2001) 644–648.
[10] B. Kumar, L. Scanlon, R. Marsh, R. Mason, R. Higgins, R. Baldwin, Structural evolution and conductivity of PEO:$LiBF_4$–MgO composite electrolytes, Electrochimica Acta 46 (2001) 1515–1521.
[11] P. Zhang, H.P. Zhang, G.C. Li, Z.H. Li, Y.P. Wu, A novel process to prepare porous membranes comprising SnO_2 nanoparticles and P(MMA-AN) as polymer electrolyte, Electrochemistry Communications 10 (2008) 1052–1055.
[12] J.Y. Xi, X.P. Qiu, M.Z. Cui, X.Z. Tang, W.T. Zhu, L.Q. Chen, Enhanced electrochemical properties of PEO-based composite polymer electrolyte with shape-selective molecular sieves, Journal of Power Sources 156 (2006) 581–588.
[13] P.P. Prosini, P. Villano, M. Carewska, A novel intrinsically porous separator for self-standing lithium-ion batteries, Electrochimica Acta 48 (2002) 227–233.
[14] A. Nishimoto, M. Watanabe, Y. Ikeda, S. Kohjiya, High ionic conductivity of new polymer electrolytes based on high molecular weight polyether comb polymers, Electrochimica Acta 43 (1998) 1177–1184.
[15] F. Croce, G.B. Appetecchi, L. Persi, B. Scrosati, Nanocomposite polymer electrolytes for lithium batteries, Nature 394 (1998) 456–458.
[16] D.E. Fenton, J.M. Parker, P.V. Wright, Complexes of alkali metal ions with poly(ethylene oxide), Polymer 14 (1973) 589.
[17] A.S. Best, A. Ferry, D.R. MacFarlane, M. Forsyth, Conductivity in amorphous polyether nanocomposite materials, Solid State Ionics 126 (1999) 269–276.
[18] P.P. Chu, M.J. Reddy, H.M. Kao, Novel composite polymer electrolyte comprising mesoporous structured SiO_2 and PEO/Li, Solid State Ionics 156 (2003) 141–153.
[19] A.M. Stephen, K.S. Nahm, M.A. Kulandainathan, G. Ravi, J. Wilson, Nanofiller incorporated poly(vinylidene flouride-hexafluoropropylene) (PVdF-HFP) composite electrolyte for lithium batteries, Journal of Power Sources 159 (2006) 1316–1321.
[20] P.A.R.D. Jayathilaka, M.A.K.L. Dissanayake, I. Albinsson B.-E. Mellander, Effect of nanoporous Al_2O_3 on thermal, dielectric and transport properties of the (PEO)LiTFSI polymer electrolyte system, Electrochimica Acta 47 (2002) 3257–3268.
[21] Z.Y. Wen, T. Itoh, T. Uno, M. Kubo, O. Yamamoto, Thermal, electrical, and mechanical properties of composite polymer electrolytes based on cross-linked poly(ethylene oxide-*co*-propylene oxide) and ceramic filler, Solid State Ionics 160 (2003) 141–148.
[22] B. Kumar, L.G. Scanlon, Composite electrolytes for lithium rechargeable batteries, Journal of Electroceramics 5 (2001) 127–139.
[23] C.C. Yang, Study of alkaline nanocomposite polymer electrolytes based on PVA–ZrO_2–KOH, Materials Science and Engineering B 131 (2006) 256–262.
[24] J.L. Souquet, M. Levy, M. Ducholat, A single microscopic approach for ionc transport in glassy and polymer electrolytes, Solid State Ionics 70–71 (1994) 337–345.
[25] S. Ramesh, A.K. Arof, Structural, thermal and electrochemical cell characteristic of poly(vinyl chloride) based polymer electrolytes, Journal of Power Sources 99 (2001) 41–47.
[26] S. Rajendran, S.B. Ravi, P. Sivakumar, Effect of salt concentration in poly(vinyl chloride)/poly(acrylonitrile) based hybrid polymer electrolytes, Journal of Power Sources 170 (2007) 460–464.
[27] S. Ganesan, B. Muthuraaman, Vinod Mathew, J. Madhavan, P. Marumuthu, S. Austin Suthanthiraraj, Performance of a new polymer electrolyte with diphenylamine in nanocrystalline dye-sensitized solar cell, Solar Energy Materials and Solar Cells 92 (2008) 1718–1722.
[28] C.C. Yang, Synthesis and characterization of the cross-linked PVA/TiO_2 composite polymer membrane for alkaline DMFC, Journal of Membrane Science 288 (2007) 51–60.
[29] N. Vassal, E. Salmon, J.F. Fauvarque, Electrochemical properties of an alkaline solid polymer electrolyte based on P(ECH-co-EO), Electrochimica Acta 45 (2000) 1527–1532.